Numerical Study of Low-Power MPD Arcjet

Ikkoh Funaki
Japan Aerospace Exploration Agency
3-1-1 Yoshinodai, Sagamihara, Kanagawa 229-8510, Japan

Kenichi Kubota and Yoshihiro Okuno
Tokyo Institute of Technology
Yokohama, Kanagawa, 226-8502, Japan

Hiroki Sato and Takayasu Fujino
University of Tsukuba
Tsukuba, Ibaraki, 305-8573, Japan

Keywords: MPD Arcjet, MPD Thruster, Low Power, Applied Field, Numerical Simulation

Abstract

In spite of many experimental studies of low-power applied-field magnetoplasmadynamic (AFMPD) thrusters, thrust efficiencies of the past thrusters are very low. Hence, drastic improvement in thrust performance is required for AF-MPD thrusters to compete against other types of electric propulsion in a moderate power regime around 10 kW. For the optimization of AF-MPD thrusters, a numerical code for the flowfield simulation is now under development. A preliminary result shows that the code can deal with a complicated mixture of the induced and applied magnetic fields, which will lead to a combination of the self-field, swirl, Hall, as well as electrothermal accelerations.

Introduction

Following the successful development of low-power thrusters (below 10 kW), scaling up electric propulsion systems toward high power is in progress. For example, a high-power Hall thruster as great as 100 kW has been reported in current research,[1] and an arcjet of 100-kW class has been investigated in some ground experiments.[2] Among them, the highest-power electric propulsion device flew in 2002, which demonstrated a 28 kW-class ammonia arcjet. [3] Although these experiments showed the possibility of high-power Hall or arcjet thrusters, their specific impulses are limited; hence, they are not desirable for some missions. The magnetoplasmadynamic (MPD) thruster is now gaining renewed interest for high-power missions such as a manned Mars mission and large orbital transfer, which will require high Isp as well as a large thrust to power ratio. The relative simplicity, robustness, high thrust density, high power capability, and ease of mission scaling of MPD thrusters compared with other electric propulsion devices make them attractive for primary propulsion. Before realizing an MPD system, however, low thrust efficiency has to be solved. So far, only Lithium propellants seem to breakthrough the low efficiency problem, [4] but the contamination problem remains. For this reason, other propellants such as argon or hydrogen should be used. [5, 6] Although thruster optimization has been hindered by the poor understanding of energy loss mechanisms which have limited improvement efforts to empirical approaches, nowadays, computational method can also assist designing the discharge chamber of MPD thrusters.[7]

To obtain a simpler thruster design without a hollow cathode at a medium power level of 10 kW, we are now redesigning a Magnetolasmadynamic (MPD) thruster. Since the electric power of more than 200 kW is usually required for self-field MPD thrusters, the usage of applied magnetic field is considered for plasma acceleration. [8] However, optimization of the AF-MPD thruster is not an easy task because the problem includes a lot of design parameters and complicated coupling between them. So, before a challenge to get some design guidelines for applied field MPD (AF-MPD) thrusters, we are now developing a numerical code for the flow and field simulation of the AF-MPD thrusters.

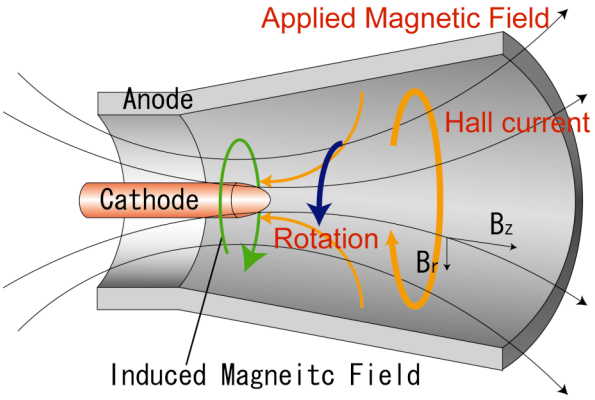

Fig.1 Principle of applied-field MPD thruster.

Applied-field MPD Thruster

Typical thruster geometry with a slowly diverging magnetic filed is schematically plotted in Fig.1. AF-MPD thruster is a hybrid accelerator using some of four processes shown below. [4,9,10,11]

1) Self-field acceleration
   A discharge current induces an azimuthal magnetic field that interacts with the discharge current. The resulting Lorentz force (***jxb***) accelerate a plasma radially inward ($j_z B_\theta$) and axially outward ($j_r B_\theta$). The axial component ($j_r B_\theta$) corresponds to an electromagnetic force. Since thrust by the self-field acceleration is proportional to J^2, where J is the discharge current, the contribution of the self-field acceleration in an AF-MPD thruster is usually small because J takes a small value.

2) Swirl acceleration
   The interaction between a discharge current and an applied magnetic field produces an electromagnetic force ($j_r B_z$, $j_z B_r$), which acts as a torque to the plasma and imparts a rotational energy to the plasma. The rotational kinetic energy can be converted into an axial kinetic energy through the gas-dynamic expansion; conserving the angular momentum and total kinetic energy of the plasma, a magnetic nozzle or a solid nozzle can accelerate the plasma in the radial direction.

3) Hall acceleration
   Under a strong applied magnetic field and a low mass flow rate, an azimuthal current (j_θ) may be induced by the interaction between the discharge current and the applied magnetic field. The product of the induced current and the applied magnetic field produces pinching ($j_\theta B_z$) and blowing ($j_\theta B_r$) forces, and the latter blowing force directly contributes to the thrust production like in the case of a self-field MPD thruster.

4) Electrothermal acceleration
   The gas is heated by the Joule heating, and its static enthalpy is converted into a kinetic energy by gas-dynamic expansion.

Depending on the thruster configuration and operational parameters of an AFMPD thruster, one should identify and then optimize the dominant acceleration process.

Numerical model and preliminary results

Physical and numerical model

We assume a plasma is axially symmetric flow and in thermal non-equilibrium. Viscosity, thermal conduction, multivalent ionization (up to Ar^{2+}), and the Hall effect are incorporated in our model. As for the magnetic field, we utilize the procedure described by Haag et al., i.e. the azimuthal induced magnetic field is solved via the induced equation, and other components (B_r and B_z) are calculated from aximuthal component of the vector potential. This method has an important advantage such that $divB = 0$ and $divA = 0$ are mathematically insured if the flowfield is assumed to be azimuthally uniform.

The thruster geometry and the magnetic field configuration used in this study are shown in Fig. 2. The thruster consists of a short cathode (8 mm in diameter and 13 mm in length) and a flared anode. The inner diameter of the anode is 28 mm at the inlet and 56 mm at the outlet. The vertical wall located at z = 45 mm is an insulator. We adopt a structured grid of 110x35 inside the thruster ($z \leq 45$ mm) and 50x60 in the plume region ($z \geq 45$ mm). Figure 2 also shows the applied magnetic field distribution. The external coil consists of 15 layers with 10 windings in each layer, and the coil current is set to 50 A. With this coil, the strength of magnetic flux density at the cathode tip is about 0.1 T. In this paper, the propellant injected from the inlet is argon, and the prescribed mass flow rate is 0.4 g/s. Since the consideration of the plasma ignition at the inlet is difficult to incorporate into the numerical simulation, we ignore the processes and assume a relatively high temperature and highly ionized plasma inflows into the thruster. The heavy particle temperature and electron temperature at the inlet are set to 8,000 K and 10,000 K respectively. Moreover we set the ionization fraction at the inlet to 0.01. In order to take account of the heat transfer from the plasma to the wall, we set the heavy particle temperature to 1,300 K on the anode surface and to 2,000 K on the cathode surface. The electron temperature is assumed to be adiabatic along the wall.

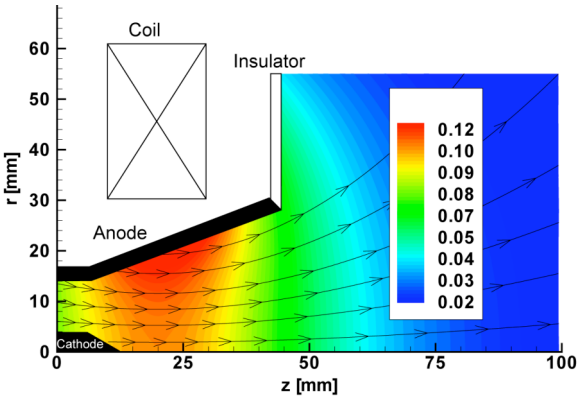

Fig.2 Thruster and magnetic field configuration.

The total discharge current J, which determines the distribution of the magnetic flux density at the inlet, is set to 1 kA. The azimuthal magnetic flux density at the inlet is obtained from the Ampere's law. As for the azimuthal magnetic flux density along the wall, it is determined from the condition that the tangential component of the electric field is zero. The vector potential on the wall is given by extrapolation for simplicity.

Preliminary results

Figure 3 shows the discharge current contour lines (axial and radial component) for both cases with and without the applied feild. The results show that the applied field causes current expansion toward the downstream region. The reason for this current expansion is considered to be the Hall effect with

regard to interaction between the azimuthal induced magnetic field, and the discharge current. Although this effect appears even in the case of self-field MPD (SF-MPD), higher total magnetic field strength due to the applied field leads to higher electron Hall parameter as shown in Fig.4.

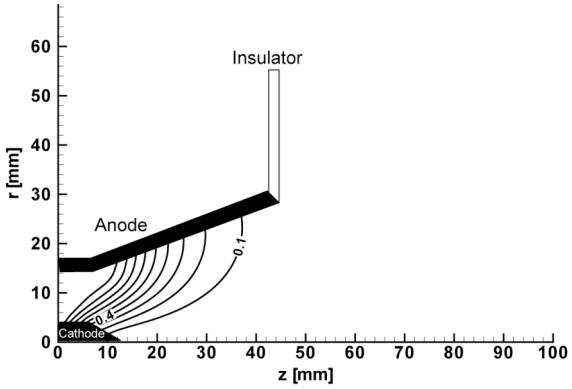

a) without applied magnetic field (only self-field)

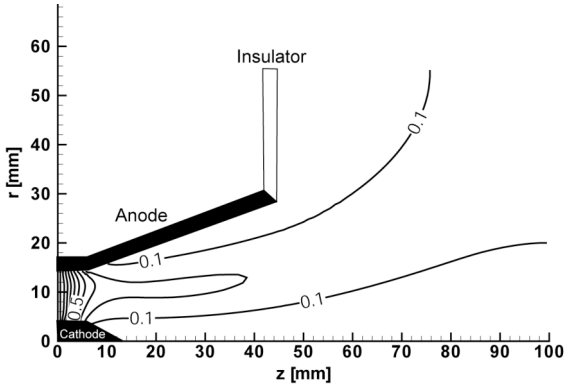

b) with applied magnetic field

Fig.3 Current contour lines.

Figure 4 describes the electron Hall parameter β_e with regard to the magnetic field strength on r-z plane, which is related with the azimuthal Hall current. Around the cathode tip, the β_e value is enhanced to more than 5, because the plasma becomes relatively rare in this region, while the β_e value tends to decrease at the point in the case of SF-MPD due to the compression effect. This density depletion at the cathode tip is mainly caused by the rotational movement of the plasma driven by the azimuthal Lorentz force the produced by the radial current and the axial applied magnetic field.

Figure 5 shows the azimuthal velocity distribution. Since the radial current density around the cathode tip is higher than that around the anode, significant azimuthal Lorentz force is produced and leads to the high azimuthal plasma velocity more than 3 km/s around the cathode tip. As the plasma flows toward downstream region, the azimuthal velocity is gradually decreased, which corresponds to the conversion of the rotational momentum into the axial momentum via the diverging nozzle.

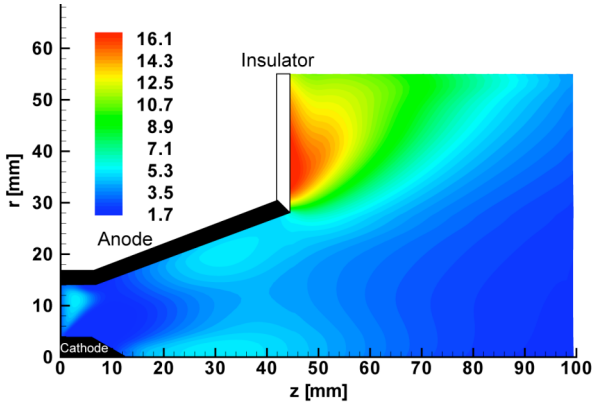

Fig.4 Hall parameter distribution.

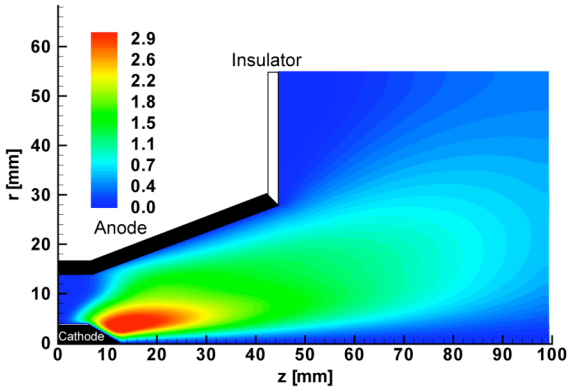

Fig.5 Induced azimuthal velocity distribution.

Summary

A preliminary numerical result of the a low-power applied-field MPD thruster is shown. It is found that the new code can deal with a complicated mixture of the induced field/flow in an applied magnetic field. To find a good 10-kW-class MPD thruster design, our next step is to check the dominant acceleration process in a variety of thruster configuration (thruster size, the ratio of anode to cathode diameter) and operational parameters such as discharge current, magnetic field strength, and mass flow rate.

Acknowledgements

This research is supported by the Grant-in-Aid for Scientific Research (B) (No.18360411) of the Japan Society for Promotion of Science, and by the center for planning and information systems in institute of space and astronautical science of Japan aerospace exploration agency.

References

[1] Jacobson, D.T., Manzella, D.H., Hofer, R.R., and Peterson, P.Y., NASA's 2004 Hall Thruster Program, *40th AIAA/ASME/SAE/ASEE Joint Propulsion Conference & Exhibition*, AIAA

2004-3600, 2004.

[2] Auweter-Kurtz, M., G-ograve, T., Habiger, H., Hammer, F., Kurtz, H., Riehle, M., and Sleziona, C., High-Power Hydrogen Arcjet Thrusters, *Journal of Propulsion and Power*, Vol.14, No.5, 1998, pp.760-773.

[3] Fife, J. M., Bromaghim, D. R., Chart, D. A., Hoskins, W. A., Vaughan, C. E., and Johnson, L. K., Orbital Performance Measurements of Air Force Electric Propulsion Space Experiment Ammonia Arcjet, *Journal of Propulsion and Power*, Vol.18, No.4, 2002, pp.749-753.

[4] Kodys, A.D., and Choueiri, E.Y., A Critical Review of the State-of-the-art in the Performance of Applied-field Magnetoplasmadynamic Thrusters, AIAA-2005-4247, *41st AIAA/ASME/SAE/ASEE Joint Propulsion Conference & Exhibition*, 2005.

[5] LaPointe, M.R., High Power MPD Thruster Development at the NASA Glenn Research Center, IEPC-2003-146, *Proceedings of 28th International Electric Propulsion Conference* (CD-ROM), Toulouse, 2003.

[6] Sovey, J.S., and Mantenieks, M.A., Performance and Lifetime Assessment of Magnetoplasmadynamic Arc Thruster Technology, *Journal of Propulsion and Power*, Vol.7, No.1, 1991, pp.71-83.

[7] Haag, D., Fertig, M., and Auweter-Kurtz, M., Numerical Simulations of Magnetoplasmadynamic Thrusters with Coaxial Applied Magnetic Field, IEPC-2007-138, *30th International Electric Propulsion Conference*, Florence, 2007.

[8] Krülle, G., Auweter-Kurtz, M., and Sasoh, A., Technology and Application Aspects of Applied Field Magnetoplasmadynamic Propulsion, *Journal of Propulsion and Power*, Vol. 14, No. 5, 1998, pp.754-763.

[9] Fradkin, D.B., Blackstock, A.W., Roehling, D.J., Stratton, T.F., Williams, M., and Liewer, K.W., Experiments Using a 25-kW Hollow Cathode Lithium Vapor MPD Arcjet, *AIAA Journal*, Vol.8, No.5, 1970, 886-894.

[10] Sasoh, A., Simple Formulation of Magnetoplasmadynamic Acceleration, *Physics of Plasmas*, Vol.1, No.3, 1994, pp.464-467.

[11] Sasoh, A., and Arakawa, Y., Thrust Formula for Applied-Field Magnetoplasmadynamic Thrusters Derived from Energy Conservation Equation, *Journal of Propulsion and Power*, Vol.11, No.2, 1995, pp.351-356.